

RESEARCH ARTICLE

Putative endogenous filovirus VP35-like protein potentially functions as an IFN antagonist but not a polymerase cofactor

Tatsunari Kondoh¹, Rashid Manzoor¹, Naganori Nao¹, Junki Maruyama¹, Wakako Furuyama¹, Hiroko Miyamoto¹, Asako Shigeno¹, Makoto Kuroda¹, Keita Matsuno^{2,3}, Daisuke Fujikura⁴, Masahiro Kajihara¹, Reiko Yoshida¹, Manabu Igarashi^{1,3}, Ayato Takada^{1,3,5*}

1 Division of Global Epidemiology, Research Center for Zoonosis Control, Hokkaido University, Sapporo, Japan, **2** Laboratory of Microbiology, Department of Disease Control, Faculty of Veterinary Medicine, Hokkaido University, Sapporo, Japan, **3** Global Station for Zoonosis Control, Global Institution for Collaborative Research and Education, Hokkaido University, Sapporo, Japan, **4** Division of Infection and Immunity, Research Center for Zoonosis Control, Hokkaido University, Sapporo, Japan, **5** School of Veterinary Medicine, the University of Zambia, Lusaka, Zambia

* atakada@czc.hokudai.ac.jp



OPEN ACCESS

Citation: Kondoh T, Manzoor R, Nao N, Maruyama J, Furuyama W, Miyamoto H, et al. (2017) Putative endogenous filovirus VP35-like protein potentially functions as an IFN antagonist but not a polymerase cofactor. PLoS ONE 12(10): e0186450. <https://doi.org/10.1371/journal.pone.0186450>

Editor: Jens H. Kuhn, Division of Clinical Research, UNITED STATES

Received: June 16, 2017

Accepted: October 2, 2017

Published: October 17, 2017

Copyright: © 2017 Kondoh et al. This is an open access article distributed under the terms of the [Creative Commons Attribution License](https://creativecommons.org/licenses/by/4.0/), which permits unrestricted use, distribution, and reproduction in any medium, provided the original author and source are credited.

Data Availability Statement: All relevant data are within the paper and its Supporting Information file.

Funding: This work was supported by Japan Society for the Promotion of Science (JSPS), Grant number 16J04404, <https://www.jsps.go.jp/english/index.html> (T.K. received this funding); Japan Initiative for Global Research Network on Infectious Diseases (J-GRID), Grant number 15FM0108008H0001, <http://www.amed.go.jp/en/>

Abstract

It has been proposed that some non-retroviral RNA virus genes are integrated into vertebrate genomes. Endogenous filovirus-like elements (EFLs) have been discovered in some mammalian genomes. However, their potential roles in ebolavirus infection are unclear. A filovirus VP35-like element (mIEFL35) is found in the little brown bat (*Myotis lucifugus*) genome. Putative mIEFL35-derived protein (mIEFL35p) contains nearly full-length amino acid sequences corresponding to ebolavirus VP35. Ebola virus VP35 has been shown to bind double-stranded RNA, leading to inhibition of type I interferon (IFN) production, and is also known as a viral polymerase cofactor that is essential for viral RNA transcription/replication. In this study, we transiently expressed mIEFL35p in human kidney cells and investigated its biological functions. We first found that mIEFL35p was coimmunoprecipitated with itself and ebolavirus VP35s but not with the viral nucleoprotein. Then the biological functions of mIEFL35p were analyzed by comparing it to ebolavirus VP35s. We found that the expression of mIEFL35p significantly inhibited human IFN- β promoter activity as well as VP35s. By contrast, expression of mIEFL35p did not support viral RNA transcription/replication and indeed slightly decrease the reporter gene expression in a minigenome assay. These results suggest that mIEFL35p potentially acts as an IFN antagonist but not a polymerase cofactor.

Introduction

Ebolaviruses are members of the family *Filoviridae* and cause severe hemorrhagic fever in humans and nonhuman primates. Five distinct species are known in the genus *Ebolavirus*: *Zaire ebolavirus*, *Sudan ebolavirus*, *Tai Forest ebolavirus*, *Bundibugyo ebolavirus*, and *Reston*

[program/list/01/06/023.html](http://www.jst.go.jp/global/english/index.html) (A.T. received this funding); Science and Technology Research Partnership for Sustainable Development (SATREPS), Grant number 15JM0110005H0004, <http://www.jst.go.jp/global/english/index.html> (A.T. received this funding); JSPS and the Ministry of Education, Culture, Sports, Science and Technology (MEXT), Grant numbers 16H02627 and 15H01249, <https://www.jsp.go.jp/english/index.html>, <http://www.mext.go.jp/en/> (A.T. received this funding). The funders had no role in study design, data collection and analysis, decision to publish, or preparation of the manuscript.

Competing interests: The authors have declared that no competing interests exist.

ebolavirus, represented by Ebola virus (EBOV), Sudan virus (SUDV), Taï Forest virus (TAFV), Bundibugyo virus (BDBV), and Reston virus (RESTV), respectively. RESTV has never caused lethal infection in humans. Filoviruses infect a variety of cell types *in vitro* [1–6], and several cellular factors have been shown to be involved in filovirus replication in host cells [7, 8]. However, the details of the mechanisms underlying the cell tropism and pathogenicity of filoviruses have not been fully elucidated yet.

It has been reported that some non-retroviral RNA virus gene sequences are found in vertebrate genomes [9, 10]. Although the biological significance of these genomic sequences is largely unknown, it was particularly noted that expression of an endogenous bornavirus-like nucleoprotein element (EBLN) found in the ground squirrel genome, which is one of such host genomic sequences, conferred resistance of oligodendroglia cells to the virus infection [11]. Recent studies have further reported that transcription of human EBLN-1 is responsible for regulating gene expression of host cells [12–14]. These observations suggest that the expression of EBLNs has some beneficial roles like endogenous retroviruses in animal genomes (e.g., *syncytin-1* and *-2*, *syncytin-A*, *-B*) [15–17]. On the other hand, hyperexpression of an endogenous retrovirus, multiple sclerosis-associated retrovirus (MSRV) whose envelope gene shares >93% similarity with *syncytin-1*, is thought to be involved in multiple sclerosis [18, 19]. It has also been reported that the expression of *syncytin-1* or the MSRV envelope protein in astrocytes or peripheral blood mononuclear cells is associated with a proinflammatory and autoimmune cascade [20, 21]. These observations suggest that endogenous retroviruses have a variety of effects on cell physiology.

Endogenous filovirus-like elements (EFLs) have also been discovered in several mammalian (e.g., tarsier, opossum, mouse, rat, and bat) genomes [10, 22–24], however, the potential roles of EFLs in the ebolavirus replication have not been elucidated. It is speculated that some of the EFLs (mEFLN, mEFL35, saEFLN, and meEFLN) have been present in the host genome for over 20 million years [10] and the presence of EFLs in host genomes may suggest a correlation with cellular susceptibility to ebolavirus infection [10, 22]. Of these EFLs, an endogenous filovirus VP35-like element found in the little brown bat (*Myotis lucifugus*), mEFL35, has a nearly full-length open reading frame (ORF) corresponding to the VP35 gene [10]. EBOV VP35 has been shown to bind double-stranded RNA (dsRNA) and inhibit type I interferon (IFN) production [25]. IFNs are a group of signaling proteins released from host cells in response to the presence of several pathogens. Viral infections commonly induce production of type I IFNs, which interfere with viral replication in infected cells, resulting in the restriction of virus propagation. EBOV replication was also shown to be inhibited by the IFN response induced by the retinoic acid-inducible gene-I (RIG-I) activation in cell culture [26]. It has been shown that ebolavirus VP35s impair human IFN- β promoter activation by inhibiting the function of RIG-I, IFN- β promoter stimulator 1 (IPS-1), and TANK-binding kinase 1 (TBK1) [27]. Furthermore, EBOV possessing VP35 with reduced ability to bind dsRNA is significantly attenuated in mice [28]. Thus, VP35s have been thought to be an important factor in the pathogenesis of ebolavirus infection. In addition to its function as an IFN inhibitor, VP35 is known as an essential cofactor in the viral polymerase complex of ebolaviruses [29]. Four viral proteins: nucleoprotein (NP), VP35, VP30, and RNA-dependent RNA polymerase (L) are major structural components of the nucleocapsid complex and are involved in viral replication and transcription [29, 30]. VP35 interacts with NP and L in this complex and both VP35-NP and VP35-L interactions are believed to be essential for viral RNA synthesis [29, 31–34].

To investigate potential functions of mEFL35, we constructed plasmids expressing putative mEFL35-derived protein (mEFL35p) in cultured cells and performed functional analyses to evaluate the potential of mEFL35p as an IFN antagonist and/or polymerase cofactor. Here we show that mEFL35p, as is the case with EBOV VP35, inhibits the RIG-I-mediated signaling

pathway and the production of IFN-β but does not act as a polymerase cofactor or dominant negative inhibitor.

Results

mIEFL35p and ebolavirus VP35s partially share the primary structure

We first confirmed that mIEFL35p showed sequence similarities to ebolavirus VP35s with low expectation values with the highest score given by RESTV VP35 (Table 1). We then compared amino acid residues involved in three subdomains mapped on the EBOV and RESTV VP35 sequences [31, 33–36]: the N-terminal domain containing the NP binding peptide (NPBP) at amino acid positions 20–48, the middle oligomerization domain at amino acid positions 82–118 which is required for VP35 homo-oligomerization, and the C-terminal domain, which is called the IFN inhibitory domain (IID), at amino acid positions 220–340 (Fig 1). We found that mIEFL35p completely lacked NPBP in the N-terminal domain. Basic amino acid residues at positions 222, 225, 248, and 251 (EBOV numbering) consisting of the first basic patch (FBP) region which is important for the polymerase cofactor activity [31] were not conserved. Furthermore, of the nine amino acids (i.e., positions 225, 235, 239, 248, 251, 282, 283, 298, and 300) which have been shown to play a critical role in the polymerase cofactor activity [31, 36], only two residues at position 239 and 283 (EBOV numbering) were conserved. Cysteine residues are frequently conserved among evolutionary related proteins that have similar structures [37]. Interestingly, despite the fact that BLASTP hit the Ebola virus VP35 (Table 1), four of the five cysteine residues at positions 135, 247, 275, and 326 (EBOV numbering), were not conserved. On the other hand, leucine residues at positions 93 and 107 (EBOV numbering), both of which are important for VP35 homo-oligomerization [35], were conserved among these proteins. Four (i.e., positions 312, 319, 322, and 339) of the six amino acid residues forming the dsRNA binding site of the IID (e.g., the central basic patch (CBP)) were conserved. These findings suggested that mIEFL35p might lack the ability to interact with NP and might limit the ability to work as a polymerase cofactor, but have a similar biological function to VP35 as an IFN antagonist.

mIEFL35p and VP35s have homo- and hetero-oligomerization potential

We transfected human embryonic kidney (HEK) 293T cells with the plasmids expressing mIEFL35p and VP35s of EBOV and RESTV and investigated the expression of these proteins by western blotting and immunofluorescence assays (Fig 2A and 2B). A 30 kDa protein, corresponding to the expected molecular weight of mIEFL35p, was detected by western blotting. In transfected cells, mIEFL35p was detected in the cytoplasm like VP35s and their intracellular localization appeared to be similar. Next, HEK 293T cells were cotransfected with the

Table 1. BLAST search data of mIEFL35.

Program	Query	Database	Subject (Accession Number)	Score	Query cover	E-value [†]	Identity
NCBI BLASTX	mIEFL35	Non-redundant protein sequences	RESTV VP35 (ACT22800)	125	93%	3e ⁻³⁰	32%
NCBI BLASTX	mIEFL35	Non-redundant protein sequences	TAFV VP35 (YP_003815424)	104	92%	3e ⁻²²	30%
NCBI BLASTX	mIEFL35	Non-redundant protein sequences	SUDV VP35 (ACR33188)	102	93%	7e ⁻²²	31%
NCBI BLASTX	mIEFL35	Non-redundant protein sequences	BDBV VP35 (AGL73451)	102	91%	1e ⁻²¹	33%
NCBI BLASTX	mIEFL35	Non-redundant protein sequences	EBOV VP35 (AKC36417)	102	79%	1e ⁻²¹	33%
NCBI BLASTP	mIEFL35p	PDB	EBOV VP35 (3FKE_A)	84.3	40%	4e ⁻²⁰	38%

[†]E-value: Expectation-value

<https://doi.org/10.1371/journal.pone.0186450.t001>

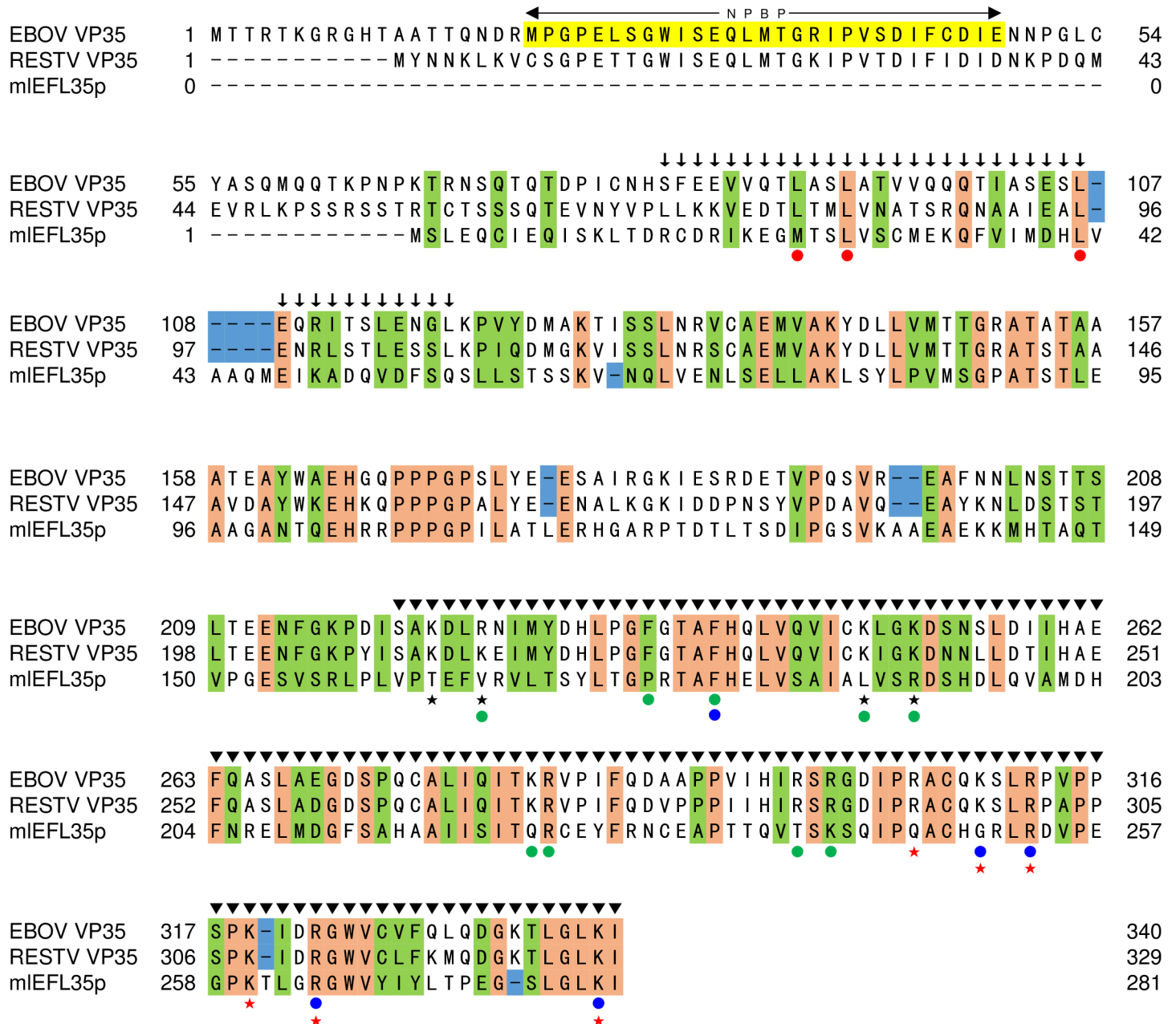


Fig 1. Comparison of primary structures of mIEFL35p and ebolavirus VP35s. The same amino acid residues that are found in VP35s and mIEFL35p are highlighted in orange. Residues highlighted in green represent amino acids that are grouped together in the same classes, based on their physical/chemical properties. The blue rectangles show sequence gaps found between mIEFL35 and VP35s. The NP binding domain consisting of the residues 20–48 (EBOV numbering), termed NPBP, is highlighted in yellow. Amino acid residues indicated by red dots have been identified to be important for VP35 homo-oligomerization as well as viral replication and transcription [35]. Amino acid residues indicated by blue dots and green dots have been shown to be critical for the dsRNA binding and polymerase cofactor activities, respectively [31, 36]. The VP35 homo-oligomerization domain and IFN inhibitory domain are indicated by arrows and arrowheads, respectively. Asterisks indicate cysteine residues in VP35s. Black and red stars indicate the amino acids that form the FBP and the CBP regions on 3-dimensional structure of the VP35 IID, respectively.

<https://doi.org/10.1371/journal.pone.0186450.g001>

expression plasmids for HA- or FLAG-tagged mIEFL35, VP35s and/or NP and solubilized proteins were immunoprecipitated with each HA-tagged protein. Consistent with previous reports [31, 33], we found that FLAG-tagged VP35s were coimmunoprecipitated with HA-

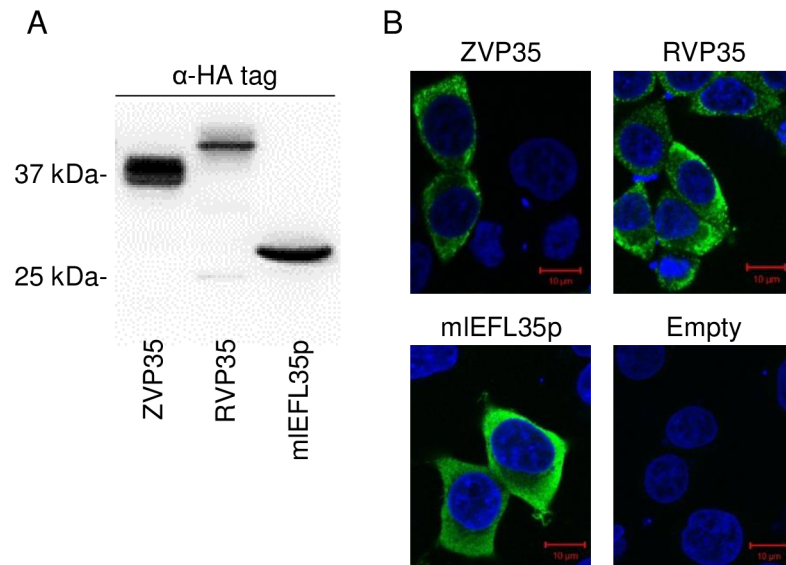


Fig 2. Expression of the mIEFL35p and VP35s in HEK 293T cells. (A) Expression of each protein was confirmed by western blotting. HA-tagged mIEFL35p (HA-mIEFL35p), HA-tagged EBOV VP35 (HA-ZVP35) and HA-tagged RESTV VP35 (HA-RVP35) were detected as 30, 37, and 40 kDa proteins, respectively. (B) Distribution of each protein is visualized by an immunofluorescence assay with anti-HA antibodies. Cells were counterstained with DAPI.

<https://doi.org/10.1371/journal.pone.0186450.g002>

tagged VP35s irrespective of the ebolavirus species, confirming their homo-oligomerization potential (Fig 3A). Interestingly, FLAG-tagged mIEFL35p was coimmunoprecipitated with not only HA-tagged mIEFL35p but also the HA-tagged VP35s of EBOV and RESTV (Fig 3A). We further analyzed the interactions of mIEFL35p with ebolavirus NPs and found that EBOV and RESTV NPs were coimmunoprecipitated with the HA-tagged VP35s of the respective viruses but not with HA-tagged mIEFL35p (Fig 3B). Taken together, these results indicated that mIEFL35p, like VP35s, had the ability of homo-oligomerization, which might be required for fundamental functions of VP35. However, consistent with its primary structure, mIEFL35p lacked the ability to interact with NP.

mIEFL35p functions as an antagonist that inhibits the RIG-I-mediated signaling pathway

The human IFN- β promoter is known to be activated through RIG-I, IPS-1, and TBK1 (Fig 4A) [27]. Using a reporter assay with these activators, the anti-IFN activity of mIEFL35p was evaluated by comparing it to influenza A virus NS1 (IAV NS1), EBOV VP35 and RESTV VP35, all of which are known to act as IFN antagonists (Fig 4B and 4C) [25, 38]. When the human IFN- β promoter activation was induced by RIG-I, mIEFL35p suppressed the IFN- β promoter activity as efficiently as EBOV VP35, but not as well as NS1. IPS-1-triggered IFN- β promoter activation was also inhibited by mIEFL35p at a similar extent to EBOV VP35. Ebolavirus VP35s and mIEFL35p showed similar effects on TBK1-induced IFN- β promoter activity. We then quantified IFN- β in supernatants of transfected cells (Fig 4B and 4D). Consistent with the results of the reporter assay, the concentrations of IFN- β released into the culture supernatant were also decreased in the presence of mIEFL35p. Although a statistically significant difference was observed only between IPS-1-triggered and control cells in the multiple comparison analysis, the expression of mIEFL35p reduced the production of IFN- β

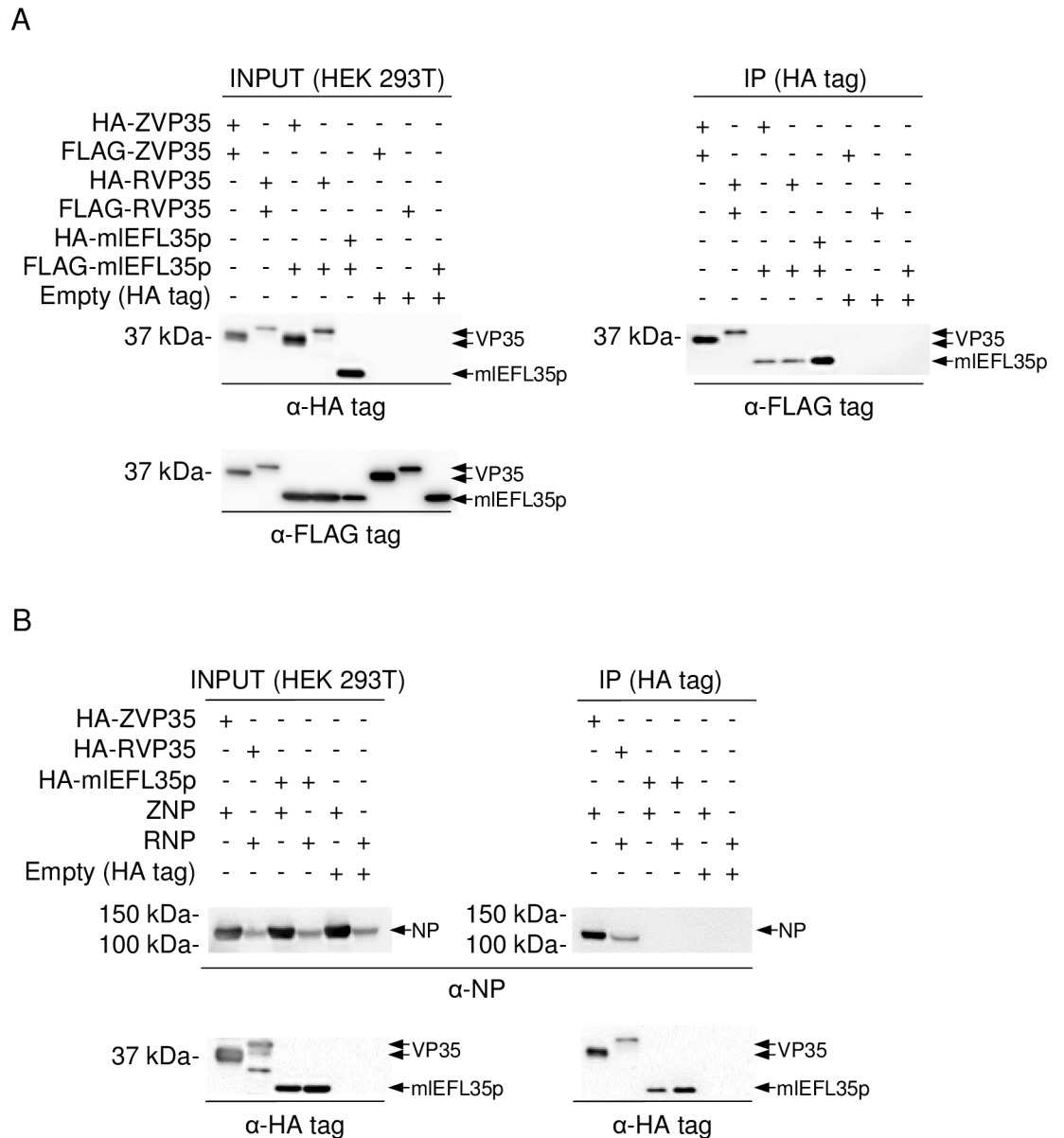


Fig 3. Immunoprecipitation assay of mIEFL35p, VP35s and NP. (A) To examine whether mIEFL35p interacted with mIEFL35p itself, EBOV and RESTV VP35s, FLAG-tagged mIEFL35p, EBOV and RESTV VP35s (FLAG-ZVP35 and FLAG-RVP35, respectively) expressed in HEK 293T cells were immunoprecipitated (IP) with HA-tagged mIEFL35p and VP35s of EBOV and RESTV (HA-ZVP35 and HA-RVP35, respectively). Precipitated proteins were detected by western blotting with anti-FLAG tag antibodies. **(B)** EBOV NP (ZNP) and RESTV NP (RNP) were expressed in HEK 293T cells and immunoprecipitated with HA-tagged VP35 of EBOV and RESTV (HA-ZVP35 and HA-RVP35) or HA-tagged mIEFL35p. HA-tagged proteins were detected by western blotting with an anti HA-tag antibody. ZNP and RNP were similarly detected with rabbit antisera specific to NPs.

<https://doi.org/10.1371/journal.pone.0186450.g003>

significantly or nearly significantly (IPS-1 or TBK1, respectively) when comparisons were made individually between mIEFL35a-expressing cells and negative control cells (Empty). It was noted that the difference in the suppression efficiency between mIEFL35p and VP35s was correlated with that seen in the reporter assay. These results suggested that mIEFL35p could have a potential function as an IFN antagonist.

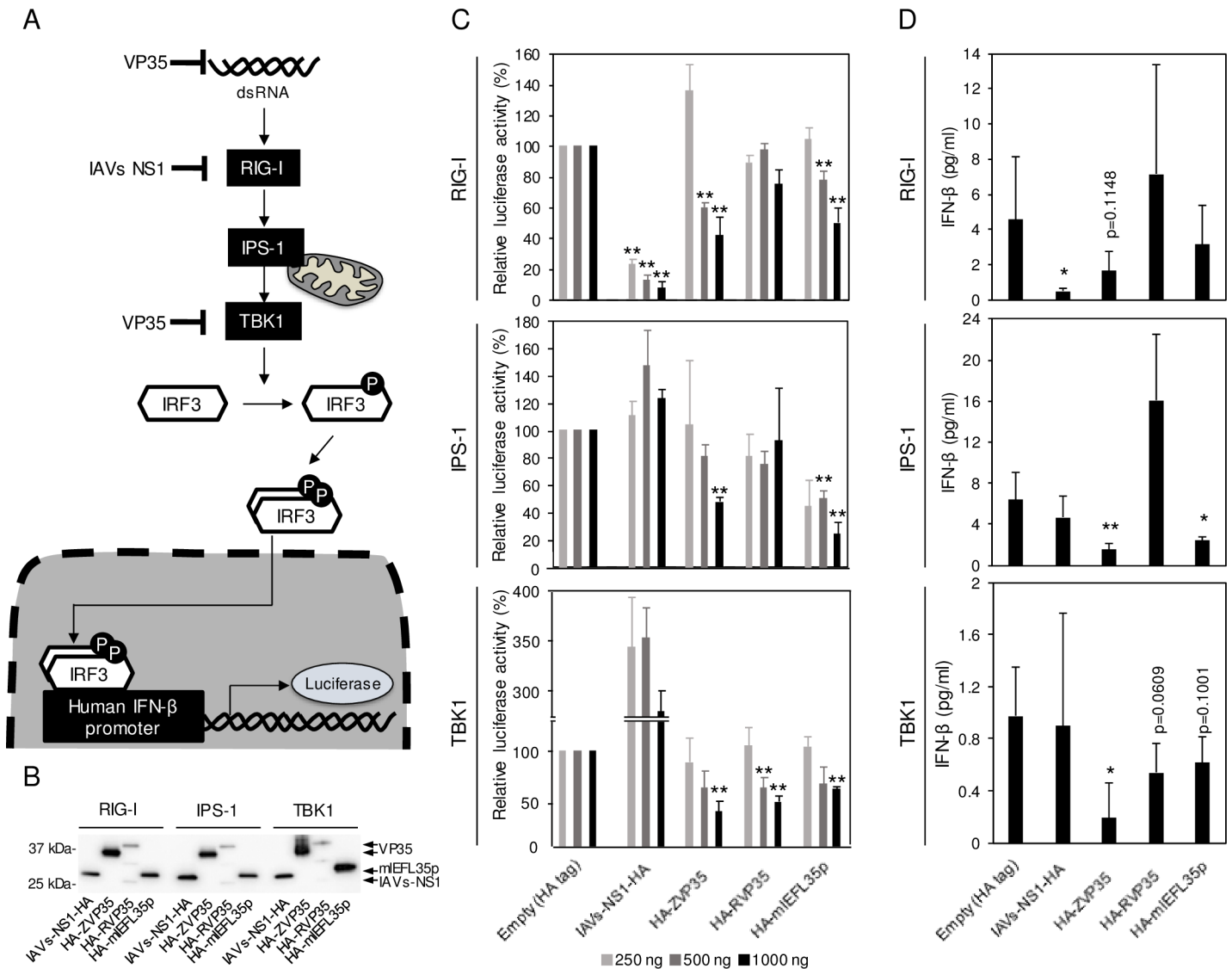


Fig 4. Inhibition of the RIG-I-mediated signaling pathway by mIEFL35p and VP35s. (A) The RIG-I-mediated signaling pathway is shown. The human IFN-β promoter is activated through RIG-I, IPS-1 and TBK1. The IFN-β promoter activity was measured by luciferase reporter assays. (B) HEK 293 cells were transfected with each plasmid expressing HA-tagged influenza A virus NS1 (IAVs-NS1-HA), EBOV VP35 (HA-ZVP35), RESTV VP35 (HA-RVP35) or mIEFL35p (HA-mIEFL35p) and the plasmids for the reporter gene expression along with the RIG-I CARD domain vector, IPS-1 or TBK1 expression vector. NS1 and VP35 are known as IFN antagonists. Western blotting was performed to examine the expression of NS1, VP35s, and mIEFL35p. Each HA-tagged protein (IAVs-NS1-HA, HA-ZVP35, HA-RVP35, and HA-mIEFL35p) was detected with an anti-HA-tag antibody. (C) Transfected cells were solubilized and luciferase assays were performed. Relative luciferase activities were calculated by setting the values given by the cells transfected with a control empty plasmid expressing the HA tag alone. Significantly lower values compared to control cells (Empty) are indicated by asterisks (* $p < 0.05$, ** $p < 0.01$). (D) Concentrations of IFN-β in the supernatants of cells transfected with the indicated plasmids (1000 ng) were measured by ELISA. Means and standard deviations of five independent experiments are shown. Significantly lower values compared to control cells (Empty) are indicated by asterisks (* $p < 0.05$, ** $p < 0.01$).

<https://doi.org/10.1371/journal.pone.0186450.g004>

mIEFL35p plays a limited role in EBOV genome transcription/replication

We used the EBOV minigenome system [29] to analyze effects of the mIEFL35p expression on EBOV genome transcription/replication (Fig 5). We first confirmed that EBOV VP35 was required for luciferase expression in this system and then found that the expression of mIEFL35p, in place of EBOV VP35, induced only background levels of luciferase activity given

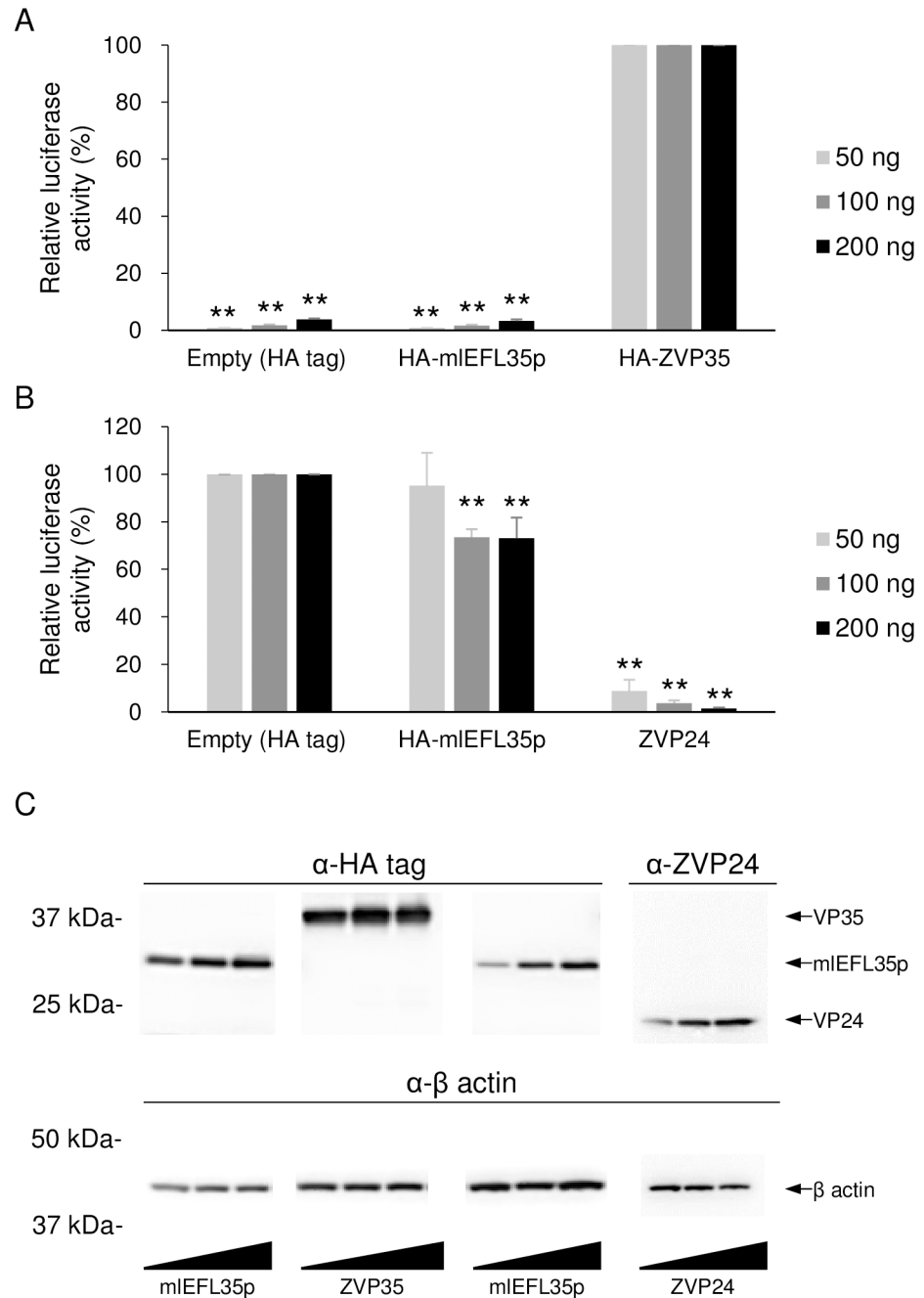


Fig 5. Luciferase expression from the Ebola virus minigenome with mIEFL35p. (A) HEK 293T cells were transfected with the indicated amounts of plasmids for the expression of the HA tag alone, HA-tagged mIEFL35p (HA-mIEFL35p), or EBOV VP35 (HA-ZVP35) along with plasmids for the expression of NP, VP30, L, the T7 polymerase and p3E5E-luc. Relative luciferase activities were determined by setting the values of control cells transfected with the HA-ZVP35-expressing plasmid to 100%. Means and standard deviations of three independent experiments are shown. Significant differences from control cells (HA ZVP35) are indicated by asterisks ($*p < 0.05$). Between the empty control and mIEFL35p, there was no significant difference. (B) HEK 293T cells were transfected with the indicated amounts of plasmids for the expression of the HA tag alone, HA-tagged mIEFL35p (HA-mIEFL35p), or EBOV VP24 (ZVP24) along with plasmids for the expression of NP, VP35, VP30, L, the T7 polymerase and p3E5E-luc. ZVP24 was used as a positive control. Means and standard deviations of three independent experiments are shown. Significantly lower values compared to control cells (Empty) are indicated by asterisks ($**p < 0.01$). (C) Expression of each protein was detected by western blotting. HA-tagged proteins (HA-ZVP35 and HA-mIEFL35p) were detected with an anti-HA tag antibody. ZVP24 were detected with a VP24-specific mouse antiserum produced with the synthetic peptide

corresponding to amino acid positions 3–15 (KATGRYNLISPKK) of EBOV VP24. β actin were detected with an anti- β actin antibody.

<https://doi.org/10.1371/journal.pone.0186450.g005>

by the empty plasmid (Fig 5A). We further examined the dominant negative effects by overexpression of mEFL35p (Fig 5B). We found that the expression of EBOV VP24 caused a significant decrease in luciferase activity as shown previously [39]. By contrast, the expression of mEFL35p only slightly reduced the luciferase activity. Expression levels of the HA-tagged proteins in the transfected cell lysates were analyzed by western blotting (Fig 5C). These results suggested that mEFL35p might not function as a polymerase cofactor or dominant negative inhibitor in this human cell line.

Discussion

In this study, we determined the mEFL35-encoding ORF sequence in the genome of the little brown bat, and biologically analyzed the potential functions of the putative protein, mEFL35p. Comparison of the amino acid sequences between mEFL35p and VP35s revealed that the primary structure of mEFL35p showed high similarity to ebolavirus VP35s. We found that mEFL35p lacked the NPBP in the N-terminal domain, whereas several amino acid residues important for VP35 homo-oligomerization and the IFN antagonist function were conserved between mEFL35p and VP35s. Accordingly, we demonstrated that mEFL35p had the potential to act as an IFN antagonist but not a polymerase cofactor.

As expected from the primary structure (i.e., conserved leucine residues at positions 93 and 107, 4 conserved residues in the CBP), mEFL35p was coimmunoprecipitated with homologous (mEFL35p) and heterologous (VP35) molecules, suggesting its homo- and hetero-oligomerization potential. It has been shown that homo-oligomerization of EBOV VP35 is important for its IFN antagonist activity [35]. Our data may also suggest a link between homo-oligomerization of mEFL35p and its function as an IFN antagonist. In addition, the ability of mEFL35p to interact with both EBOV and RESTV VP35s strongly suggested that mEFL35p and VP35s have structural similarity and share some functions. Interestingly, mEFL35p inhibited the RIG-I-mediated IFN- β production more efficiently than RESTV VP35 and its inhibitory potential was indeed similar to that of EBOV VP35. Although the expression level of RVP35 seemed to be lower than those of ZVP35 and mEFL35p, since TBK1-triggered IFN- β promoter activation was inhibited as efficiently as ZVP35, it is not highly likely that the low expression of RVP35 was a major cause of less inhibitory potential. However, there is no difference between EBOV and RESTV VP35s in the amino acid residues that are critical for VP35 homo-oligomerization and the dsRNA binding site, both of which are required for the IFN antagonist activity of VP35s [35, 40]. Leung et al. [41] reported that RESTV VP35 contained an additional helical structure in its IFN inhibitory domain and proposed that the helical structure might increase the stability and decrease the flexibility of the RESTV VP35 molecule. Such a structural difference might influence the IFN antagonist activity. On the other hand, Guito et al. [42] demonstrated that both EBOV and RESTV VP35s were similarly potent IFN antagonist proteins. Since differences in experimental conditions (e.g., use of a human codon-optimized ORF of VP35 and different procedures for IFN induction) might cause different effects, further studies are required to clarify whether anti-IFN potential is involved in the differential pathogenicity of EBOV and RESTV.

It has been demonstrated that VP35 interacts with IRF kinases such as TBK1 and inhibitor of κ B kinase epsilon (IKK ϵ) and the physical interaction between IKK ϵ and either IPS-1, IRF-3, or IRF-7 was impaired by EBOV VP35 overexpression [43]. As shown in Fig 4, our reporter assay showed that TBK1-induced human IFN- β promoter activity was most significantly inhibited by mEFL35p, suggesting that mEFL35p also targets these IRF kinases. EBOV VP35

binds not only dsRNA but also PKR activator (PACT), both of which are recognized by RIG-I. The ability of VP35 to block the PACT activation requires the CBP structure [44]. Comparison of primary structure between mEFL35p and ebolavirus VP35s (Fig 1) indicates that majority of amino acids forming the CBP structure are conserved in mEFL35p. This suggests that mEFL35p may also inhibit the PACT activation like EBOV P35.

It was noted that four of the five cysteine residues in VP35s were not conserved in mEFL35p. Cysteine residues often form a disulphide bond that plays an important role in protein folding and stability. Thus, cysteine residues important for protein structures are generally conserved among related proteins [37]. Crystal structure analysis has shown that the cysteine residues at positions 247 and 275 of EBOV VP35 do not form a disulfide bond [45]. Although the structural impacts of the other cysteine residues of VP35 remain unknown, our data suggest that cysteine residues of mEFL35p and VP35s are not important for the fundamental function as an IFN antagonist.

As suggested by the comparison of the amino acid sequences between mEFL35p and VP35s (e.g., lack of the NPBP region), NP was not coimmunoprecipitated with mEFL35p. The NP-VP35 interaction has been shown to be essential for viral transcription/replication [29]. Accordingly, our EBOV minigenome reporter assay demonstrated that mEFL35p could not be substituted for EBOV VP35 in the viral transcription/replication cycle. It was also speculated that overexpression of mEFL35p might show dominant negative effects by forming hetero-oligomers between mEFL35p and VP35 molecules. However, mEFL35p only slightly interfered with the VP35 function. These results suggested that mEFL35p might not have critical functions involved in viral transcription/replication. Further studies with chimeric proteins between mEFL35p and VP35 might provide more detailed information on specific regions required for the VP35 function as a polymerase cofactor.

It has been proposed that endogenous retroviruses in animal genomes provide some beneficial effects to host animals and might play important roles in their coevolution [46–48]. It has also been demonstrated that non-retroviral elements, EBLNs, are involved in antiviral effects and regulation of neighboring gene expression [11–13]. However, in this study, we demonstrated that mEFL35p potentially acted as an IFN antagonist like EBOV VP35, suggesting a suppressive effect on host immunity. While mEFL35 was found in an insectivorous bat (*Myotis lucifugus*), there is no information on susceptibility of this bat species to ebolaviruses. In addition, cell lines of this bat species are also unavailable. Interestingly, however, some species of fruit bats are suspected to be natural hosts [49–52]. It should also be noted that EBOV is able to replicate and lead to seroconversion without any symptoms in some insectivorous bat species [53]. Overall, previous studies have indicated that many species of bats are susceptible to ebolaviruses. To better understand the potential roles of EFLs in ebolavirus infection, it would be of interest to screen various bat cell lines for the presence of genomic EFLs and to analyze their biological effects by knockdown/knockout experiments using cell lines naturally expressing EFLs. It is reported that transcription of human EBLN-1 is responsible for regulating gene transcription [12–14]. Thus, it is also important to focus on the function of not only EFL-derived proteins but also noncoding RNA transcripts. Once cell lines naturally expressing EFLs are in hand, loss-of-function experiments are needed for further understanding of the biological significance of EFLs in the ebolavirus ecology.

Materials and methods

Bioinformatics

The nucleotide sequences of mEFL35 shown in NCBI (Accession numbers: JN847697 and JN847701) were partial ORFs. To get its full-length ORF, we obtained the genomic sequence

between the 5'-target site duplication (TSD) and 3'-TSD from the Ensemble database (<http://www.ensembl.org/index.html>) since the full-length mEFL35 ORF was reported to be located between these TSDs [9, 10]. The obtained sequence (1944 nucleotides) was analyzed using the NCBI BLASTX program in the non-redundant protein sequences database and found to contain the mEFL35 full-length ORF (S1 Text) encoding a putative mEFL35-derived protein (mEFL35p) that showed high sequence similarities to ebolavirus VP35s with low expectation values (Table 1). Next, we used the NCBI BLASTP program in the Protein Data Bank to confirm that the amino acid sequence of mEFL35p matched with the structure of EBOV VP35 (Table 1). Amino acid sequences were aligned using Clustal W [54], and then amino acids having similar physical-chemical properties were grouped.

Cell culture and construction of plasmids

HEK 293 cells (ATCC[®] CRL-1573[™]) and 293T cells (ATCC[®] CRL-3216[™]) were grown in Dulbecco's modified Eagle's medium with 10% fetal calf serum (FCS). Cells were incubated in a humidified 5% CO₂ incubator at 37°C. The cDNA encoding the mEFL35 ORF was synthesized and cloned into a pUCFa vector (FASMAC). The cDNA encoding mEFL35p fused to an HA or FLAG tag at the N terminus was cloned into the mammalian expression vector pCAGGS [55] using an In-Fusion cloning kit (BD Clontech). In a similar way, the expression plasmids for N-terminally HA- or FLAG-tagged VP35 and NP of an EBOV isolate, Mayinga (species *Zaire ebolavirus*) or a RESTV isolate, Pennsylvania (species *Reston ebolavirus*) were constructed. The ORF of the NS1 protein of influenza A virus (strain PR8) with a splice acceptor site mutation [56] was C-terminally fused with an HA tag and cloned into pCAGGS. The EBOV minigenome plasmid containing the firefly luciferase gene, p3E5E-luc [39], was also synthesized and cloned into a pUCFa vector (FASMAC). The NP, VP35, VP30, VP24, and L genes of EBOV (Mayinga) were similarly cloned into pCAGGS. Expression vectors used to provide human IPS-1 have been described previously [57]. The human TBK1 gene was also cloned into pCAGGS.

Western blotting for the detection of expressed proteins

Each cell lysate was mixed with 2 × sample buffer (Bio Rad) and incubated at 65°C for 15 min. Expressed proteins were separated in sodium dodecyl sulfate (SDS)-polyacrylamide gels (SuperSep Ace 5–20%, Wako) and transferred to polyvinylidene fluoride (PVDF) membranes (Merck). PBS containing 3% (wt/vol) skim milk (Becton Dickinson) and PBS containing 0.05% (vol/vol) Tween 20 (PBST) were used as blocking and wash buffers, respectively. PVDF membranes were incubated with an anti-HA monoclonal antibody (abcam, ab1424, 1:5000), anti-β actin monoclonal antibody (abcam, ab6276, 1:5000), or VP24-specific mouse antiserum for 60 min, washed with PBST, and then incubated with horseradish peroxidase-conjugated goat anti-mouse IgG (Jackson ImmunoResearch, 115-035-062, 1:10000) for 60 min. After washing with PBST, the bound antibodies were visualized with Immobilon Western (Millipore).

Indirect immunofluorescence assay

HEK 293T cells were seeded on 8-well chamber slides (Watson Co., Ltd) precoated with poly-L-lysine (Cultrex). One day after seeding, the cells were transfected with the plasmids encoding mEFL35p using TransIT LT1 reagent (Mirus) according to the manufacturer's instructions. At 24 hours post-transfection, the cells were fixed in 4% (wt/vol) paraformaldehyde for 15 min, and permeabilized by incubation for 5 min in PBS containing 0.4% (vol/vol) Triton X-100. The following procedures were performed at room temperature. The cells were incubated

with PBS containing 1% (wt/vol) BSA followed by incubation with the anti-HA antibody (abcam, ab1424, 1:500) for 60 min. After washing with PBST, the cells were incubated with Alexa Fluor 488-conjugated goat anti-mouse IgG (Molecular Probes, A11001) for 30 min in the dark. Nuclei were stained using 1 $\mu\text{g}/\text{ml}$ 4',6-diamidino-2-phenylindole, dihydrochloride (DAPI) (Molecular Probes) for 10 min in the dark. Images were acquired with a 63 \times oil objective lens on a Zeiss LSM700 inverted microscope and ZEN 2009 software (Carl Zeiss).

Immunoprecipitation assay

HEK 293T cells were transfected with the plasmids encoding HA- and/or FLAG-tagged VP35 and mEFL35p using TransIT LT1 reagent (Mirus) according to the manufacturer's instructions. For the NP expression, pCAGGS plasmids encoding untagged NPs were used. Two days after transfection, the cells were lysed with cold lysis buffer (50 mM Tris-HCl pH 8.0, 150 mM NaCl, 2 mM EDTA, 10% glycerol and 0.05% NP-40) containing EDTA-free protease inhibitor (Roche). To facilitate disruption of the cells, cell suspensions were frozen at -20°C . Samples were centrifuged at $10000 \times g$ at 4°C for 10 min. Supernatants were mixed with EZview Red Anti-HA Affinity Gel beads (Sigma) and incubated at 4°C overnight with gentle rocking. After washing the beads with the lysis buffer, HA-peptides (Sigma, 100 $\mu\text{g}/\text{ml}$) were mixed with them and incubated at 4°C for 15 min with gentle rocking to elute the HA-tagged protein. The beads were centrifuged at $500 \times g$ at 4°C for 1 min and the supernatant was mixed with 2 \times sample buffer (Bio Rad) and incubated at 65°C for 15 min. Precipitated proteins were separated in SDS-polyacrylamide gels (SuperSep Ace 5–20%, Wako) and transferred to PVDF membranes (Merck). HA- or FLAG-tagged mEFL35p and VP35s were detected with the anti-HA tag antibody (abcam, ab1424, 1:5000) or anti-FLAG tag antibody (Sigma, F1804, 1:5000). NPs were detected with a mixture of rabbit antiserum to EBOV NP (FS0169, 1:2000) and RESTV NP (FS0170, 1:2000) [58]. The bound antibodies were visualized with Immobilon Western (Millipore).

Reporter assay for human IFN- β promoter activity

HEK 293 cells (1×10^5) on 12-well plates were transfected with 250, 500, or 1000 ng of each plasmid expressing C-terminally HA-tagged influenza A virus NS1 (IAVs-NS1-HA), N-terminally HA-tagged EBOV VP35 (HA-ZVP35), RESTV VP35 (HA-RVP35) or mEFL35p (HA-mEFL35p) and the plasmids for the human IFN- β promoter-driven firefly luciferase reporter gene (pIFN β -luc, 250 ng, a kind gift from Sonja Best, NIH/NIAID), the Renilla luciferase-based pRL-TK vector (50 ng, Promega), along with the RIG-I caspase activation and recruitment domain (CARD) domain vector (50 ng/well, a kind gift of Sonja Best), IPS-1 expression vector (50 ng/well), or TBK1 expression vector (100 ng/well) using FuGENE HD transfection reagent (Promega) according to the manufacturer's recommendations. Twenty-four hours after transfection, cell culture supernatants were collected and centrifuged at $300 \times g$, and then the supernatants were stored at -80°C until use. These cell supernatants were subjected to Enzyme-linked immunosorbent assay (ELISA) to measure the concentrations of human IFN- β . The cells were harvested and lysed in Passive Lysis Buffer (Promega), and then luciferase assays were performed using the Dual-Luciferase Reporter Assay System (Promega) according to the manufacturer's directions. These cell lysates were subjected to SDS-polyacrylamide gels, followed by western blotting, to examine the expression of each protein. Firefly luciferase values were normalized to Renilla luciferase values. Normalized values were then compared to negative control (no induction) to obtain fold induction values. The results are presented as percent induction in comparison to the positive control (with only the HA-tag expression vector), the value for which was set to 100%.

Human IFN- β ELISA

The quantitation of IFN- β was examined with a VeriKine-HS Human Interferon Beta Serum ELISA Kit (PBL Assay Science). All procedures were performed according to protocol A of the manufacturer's instructions. The optical density at 450 nm (OD450) was measured using SoftMax[®] Pro 6.2.1 software (Molecular Devices). The standard curve was obtained by plotting the OD450, and then the concentrations of IFN- β (pg/ml) in the samples were calculated.

Minigenome reporter assay

HEK 293T cells (5×10^4) on 24-well plates were transfected with 50, 100, or 200 ng of plasmids encoding the HA tag alone, HA-ZVP35, or HA-mEFL35p, along with expression plasmids for the production of EBOV NP (50 ng), VP30 (30 ng), L (400 ng), p3E5E-luc (100 ng), and the T7 polymerase (100 ng) using the TransIT LT1 reagent (Mirus). In another experiment, HEK 293T cells (5×10^4) on 24-well plates were transfected with 50, 100, or 200 ng of plasmids encoding the HA tag alone, HA-mEFL35p, or VP24, along with expression plasmids for the production of EBOV NP (50 ng), VP35 (50 ng), VP30 (30 ng), L (400 ng), p3E5E-luc (100 ng), and the T7 polymerase (100 ng) using the TransIT LT1 reagent (Mirus). At 36 hours after transfection, the cells were lysed with Passive Lysis Buffer (Promega), and the luciferase activity was measured using the Bright-Glo luciferase assay system (Promega) according to the manufacturer's instructions. These cell lysates were also subjected to SDS-polyacrylamide gels, followed by western blot analysis to examine the expression of each protein. The firefly luciferase activity was compared to the negative control (without EBOV L expression vector) values to obtain fold luciferase activity values and relative luciferase activities were determined by setting the values of control cells to 100%.

Statistical analysis

All analyses were performed with R (version 3.2.3) [59]. One-way analysis of variance (ANOVA) was performed, followed by a post hoc paired Student's t-test with Bonferroni adjustment for multiple comparisons.

Supporting information

S1 Text. Full-length mEFL35 ORF and mEFL35p.
(DOCX)

Acknowledgments

The authors would like to thank Sonja Best (NIH/NIAID) for the pIFN β -luc and RIG-I CARD vector. We also thank Kim Barrymore for improving the English.

Author Contributions

Conceptualization: Tatsunari Kondoh, Ayato Takada.

Data curation: Tatsunari Kondoh, Asako Shigeno.

Formal analysis: Tatsunari Kondoh, Manabu Igarashi, Ayato Takada.

Funding acquisition: Tatsunari Kondoh, Ayato Takada.

Investigation: Tatsunari Kondoh, Rashid Manzoor, Naganori Nao, Daisuke Fujikura, Manabu Igarashi.

Methodology: Tatsunari Kondoh, Rashid Manzoor, Daisuke Fujikura, Manabu Igarashi, Ayato Takada.

Project administration: Ayato Takada.

Resources: Tatsunari Kondoh, Rashid Manzoor, Naganori Nao, Junki Maruyama, Hiroko Miyamoto, Asako Shigeno, Makoto Kuroda, Keita Matsuno, Daisuke Fujikura, Manabu Igarashi, Ayato Takada.

Supervision: Ayato Takada.

Validation: Tatsunari Kondoh, Rashid Manzoor, Ayato Takada.

Visualization: Tatsunari Kondoh, Masahiro Kajihara, Ayato Takada.

Writing – original draft: Tatsunari Kondoh, Ayato Takada.

Writing – review & editing: Tatsunari Kondoh, Rashid Manzoor, Naganori Nao, Junki Maruyama, Wakako Furuyama, Hiroko Miyamoto, Asako Shigeno, Makoto Kuroda, Keita Matsuno, Daisuke Fujikura, Masahiro Kajihara, Reiko Yoshida, Manabu Igarashi, Ayato Takada.

References

1. Takada A., Robison C., Goto H., Sanchez A., Murti K.G., Whitt M.A. et al. A system for functional analysis of Ebola virus glycoprotein. *Proc Natl Acad Sci U S A*. 1997; 94, 14764–14769. <https://doi.org/10.1073/pnas.94.26.14764> PMID: 9405687
2. Chan S.Y., Speck R.F., Ma M.C. and Goldsmith M.A. Distinct mechanisms of entry by envelope glycoproteins of Marburg and Ebola (zaire) viruses. *J Virol*. 2000; 74, 4933–4937. <https://doi.org/10.1128/JVI.74.10.4933-4937.2000> PMID: 10775638
3. Kash J.C., Mühlberger E., Carter V., Grosch M., Perwitasari O., Proll S.C., et al. Global suppression of the host antiviral response by Ebola- and Marburgviruses: increased antagonism of the type I interferon response is associated with enhanced virulence. *J Virol*. 2006; 80, 3009–3020. <https://doi.org/10.1128/JVI.80.6.3009-3020.2006> PMID: 16501110
4. Harcourt B.H., Sanchez A. and Offermann M.K. Ebola virus inhibits induction of genes by double-stranded RNA in endothelial cells. *Virology*. 1998; 252, 179–188. <https://doi.org/10.1006/viro.1998.9446> PMID: 9875327
5. Ebihara H., Takada A., Kobasa D., Jones S., Neumann G., Theriault S., et al. Molecular determinants of Ebola virus virulence in mice. *PLoS Pathogens*. 2006; 2. <https://doi.org/10.1371/journal.ppat.0020073> PMID: 16848640
6. Maruyama J., Miyamoto H., Kajihara M., Ogawa H., Maeda K., Sakoda Y., et al. Characterization of the envelope glycoprotein of a novel filovirus, Llovio virus. *J Virol*. 2014; 88, 99–109. <https://doi.org/10.1128/JVI.02265-13> PMID: 24131711
7. Takada A. Filovirus tropism: Cellular molecules for viral entry. *Frontiers in microbiology*. 2012; 3, 34. <https://doi.org/10.3389/fmicb.2012.00034> PMID: 22363323
8. Kajihara M. and Takada A. Host Cell Factors Involved in Filovirus Infection. *Current Tropical Medicine Reports*. 2015; 2, 30–40. <https://doi.org/10.1007/s40475-015-0039-x>
9. Horie M., Honda T., Suzuki Y., Kobayashi Y., Daito T., Oshida T., et al. Endogenous non-retroviral RNA virus elements in mammalian genomes. *Nature*. 2010; 463, 84–87. <https://doi.org/10.1038/nature08695> PMID: 20054395
10. Belyi V.A., Levine A.J. and Skalka A.M. Unexpected inheritance: Multiple integrations of ancient bornavirus and ebolavirus/marburgvirus sequences in vertebrate genomes. *PLoS Pathogens*. 2010; 6, e1001030. <https://doi.org/10.1371/journal.ppat.1001030> PMID: 20686665
11. Fujino K., Horie M., Honda T., Merriman D.K. and Tomonaga K. Inhibition of Borna disease virus replication by an endogenous bornavirus-like element in the ground squirrel genome. *Proc Natl Acad Sci U S A*. 2014; 111, 13175–13180. <https://doi.org/10.1073/pnas.1407046111> PMID: 25157155
12. Sofuku K., Parrish N.F., Honda T. and Tomonaga K. Transcription profiling demonstrates epigenetic control of non-retroviral RNA virus-derived elements in the human genome. *Cell Rep*. 2015; 12, 1548–1554. <https://doi.org/10.1016/j.celrep.2015.08.007> PMID: 26321645

13. He P., Sun L., Zhu D., Zhang H., Zhang L., Guo Y.J., et al. Knock-down of endogenous bornavirus-like nucleoprotein 1 inhibits cell growth and induces apoptosis in human oligodendroglia cells. *Int J Mol Sci.* 2016; 17. <https://doi.org/10.3390/ijms17040435> PMID: 27023521
14. Myers KN, Barone G, Ganesh A, Staples CJ, Howard AE, Beveridge RD, et al. The bornavirus-derived human protein EBLN1 promotes efficient cell cycle transit, microtubule organisation and genome stability. *Sci Rep.* 2016; 6:35548. <https://doi.org/10.1038/srep35548> PMID: 27739501
15. Mi S, Lee X, Li X, Veldman GM, Finnerty H, Racie L, et al. Syncytin is a captive retroviral envelope protein involved in human placental morphogenesis. *Nature.* 2000; 403(6771):785–9. <https://doi.org/10.1038/35001608> PMID: 10693809.
16. Blaise S, de Parseval N, Benit L, Heidmann T. Genomewide screening for fusogenic human endogenous retrovirus envelopes identifies *syncytin 2*, a gene conserved on primate evolution. *Proc Natl Acad Sci U S A.* 2003; 100(22):13013–8. <https://doi.org/10.1073/pnas.2132646100> PMID: 14557543
17. Dupressoir A, Marceau G, Verochet C, Benit L, Kanellopoulos C, Sapin V, et al. *Syncytin-A* and *syncytin-B*, two fusogenic placenta-specific murine envelope genes of retroviral origin conserved in Muridae. *Proc Natl Acad Sci U S A.* 2005; 102(3):725–30. <https://doi.org/10.1073/pnas.0406509102> PMID: 15644441
18. Mameli G, Astone V, Arru G, Marconi S, Lovato L, Serra C, et al. Brains and peripheral blood mononuclear cells of multiple sclerosis (MS) patients hyperexpress MS-associated retrovirus/HERV-W endogenous retrovirus, but not Human herpesvirus 6. *J Gen Virol.* 2007; 88(Pt 1):264–74. <https://doi.org/10.1099/vir.0.81890-0> PMID: 17170460.
19. Machnik G, Skudrzyk E, Buldak L, Labuzek K, Ruczynski J, Alenowicz M, et al. A Novel, Highly Selective RT-QPCR Method for Quantification of MSRV Using PNA Clamping Syncytin-1 (ERVWE1). *Molecular biotechnology.* 2015; 57(9):801–13. <https://doi.org/10.1007/s12033-015-9873-2> PMID: 25976174
20. Rolland A, Jouvin-Marche E, Viret C, Faure M, Perron H, Marche PN. The envelope protein of a human endogenous retrovirus-W family activates innate immunity through CD14/TLR4 and promotes Th1-like responses. *J Immunol.* (Baltimore, Md: 1950). 2006; 176(12):7636–44. PMID: 16751411.
21. Antony JM, Ellestad KK, Hammond R, Imaizumi K, Mallet F, Warren KG, et al. The human endogenous retrovirus envelope glycoprotein, syncytin-1, regulates neuroinflammation and its receptor expression in multiple sclerosis: a role for endoplasmic reticulum chaperones in astrocytes. *J Immunol.* (Baltimore, Md: 1950). 2007; 179(2):1210–24. PMID: 17617614.
22. Taylor D.J., Leach R.W. and Bruenn J. Filoviruses are ancient and integrated into mammalian genomes. *BMC Evol Biol.* 2010; 10, 193. <https://doi.org/10.1186/1471-2148-10-193> PMID: 20569424
23. Taylor D.J., Dittmar K., Ballinger M.J. and Bruenn J.A. Evolutionary maintenance of filovirus-like genes in bat genomes. *BMC Evol Biol.* 2011; 11. <https://doi.org/10.1186/1471-2148-11-336> PMID: 22093762
24. Taylor D.J., Ballinger M.J., Zhan J.J., Hanzly L.E. and Bruenn J.A. Evidence that ebolaviruses and cuevaviruses have been diverging from marburgviruses since the Miocene. *PeerJ.* 2014; 2. <https://doi.org/10.7717/peerj.556> PMID: 25237605
25. Cardenas W.B., Loo Y.M., Gale M., Hartman A.L., Kimberlin C.R., Martinez-Sobrido L., et al. Ebola virus VP35 protein binds double-stranded RNA and inhibits alpha/beta interferon production induced by RIG-I signaling. *J Virol.* 2006; 80, 5168–5178. <https://doi.org/10.1128/JVI.02199-05> PMID: 16698997
26. Spiropoulou C.F., Ranjan P., Pearce M.B., Sealy T.K., Albarino C.G., Gangappa S., et al. RIG-I activation inhibits ebolavirus replication. *Virology.* 2009; 392, 11–15. <https://doi.org/10.1016/j.virol.2009.06.032> PMID: 19628240
27. Basler C.F. and Amarasinghe G.K. Evasion of Interferon Responses by Ebola and Marburg Viruses. *J Interferon Cytokine Res.* 2009; 29, 511–520. <https://doi.org/10.1089/jir.2009.0076> PMID: 19694547
28. Hartman A.L., Bird B.H., Towner J.S., Antoniadou Z.-A., Zaki S.R. and Nichol S.T. Inhibition of IRF-3 activation by VP35 is critical for the high level of virulence of Ebola virus. *J Virol.* 2008; 82, 2699–2704. <https://doi.org/10.1128/JVI.02344-07> PMID: 18199658
29. Mühlberger E, Weik M., Volchkov V.E., Klenk H.D. and Becker S. Comparison of the transcription and replication strategies of Marburg virus and Ebola virus by using artificial replication systems. *J Virol.* 1999; 73, 2333–2342. PMID: 9971816
30. Elliott L.H., Kiley M.P. and McCormick J.B. Descriptive analysis of Ebola virus proteins. *Virology.* 1985; 147, 169–176. [https://doi.org/10.1016/0042-6822\(85\)90236-3](https://doi.org/10.1016/0042-6822(85)90236-3) PMID: 4060597
31. Prins K.C., Binning J.M., Shabman R.S., Leung D.W., Amarasinghe G.K. and Basler C.F. Basic residues within the ebolavirus VP35 protein are required for its viral polymerase cofactor function. *J Virol.* 2010; 84, 10581–10591. <https://doi.org/10.1128/JVI.00925-10> PMID: 20686031
32. Trunschke M., Conrad D., Enterlein S., Olejnik J., Brauburger K. and Mühlberger E. The L-VP35 and L-L interaction domains reside in the amino terminus of the Ebola virus L protein and are potential targets

- for antivirals. *Virology*. 2013; 441, 135–145. <https://doi.org/10.1016/j.virol.2013.03.013> PMID: [23582637](https://pubmed.ncbi.nlm.nih.gov/23582637/)
33. Kirchdoerfer R.N., Abelson D.M., Li S., Wood M.R. and Saphire E.O. Assembly of the Ebola virus nucleoprotein from a chaperoned VP35 complex. *Cell Rep*. 2015; 12, 140–149. <https://doi.org/10.1016/j.celrep.2015.06.003> PMID: [26119732](https://pubmed.ncbi.nlm.nih.gov/26119732/)
 34. Leung D.W., Borek D., Luthra P., Binning J.M., Anantpadma M., Liu G., et al. An intrinsically disordered peptide from Ebola virus VP35 controls viral RNA synthesis by modulating nucleoprotein-RNA interactions. *Cell Rep*. 2015; 11, 376–389. <https://doi.org/10.1016/j.celrep.2015.03.034> PMID: [25865894](https://pubmed.ncbi.nlm.nih.gov/25865894/)
 35. St Reid P., Cardenas W.B. and Basler C.F. Homo-oligomerization facilitates the interferon-antagonist activity of the ebolavirus VP35 protein. *Virology*. 2005; 341, 179–189. <https://doi.org/10.1016/j.virol.2005.06.044> PMID: [16095644](https://pubmed.ncbi.nlm.nih.gov/16095644/)
 36. Leung D.W., Prins K.C., Basler C.F. and Amarasinghe G.K. Structural basis for dsRNA recognition and interferon antagonism by Ebola VP35. *Nat Struct Mol Biol*. 2010; 1, 526–531. <https://doi.org/10.1038/nsmb.1765> PMID: [20081868](https://pubmed.ncbi.nlm.nih.gov/20081868/)
 37. Dayhoff M., Schwartz R. and Orcutt B. A Model of Evolutionary Change in Proteins. In: Dayhoff M. editor. *Atlas of protein sequence and structure*. Silver Spring: National Biomedical Research Foundation; 1978. pp. 345–352.
 38. Gack M.U., Albrecht R.A., Urano T., Inn K.-S., Huang I.-C., Camero E., et al. Influenza A virus NS1 targets the ubiquitin ligase TRIM25 to evade recognition by the host viral RNA sensor RIG-I. *Cell Host Microbe*. 2009; 5, 439–449. <https://doi.org/10.1016/j.chom.2009.04.006> PMID: [19454348](https://pubmed.ncbi.nlm.nih.gov/19454348/)
 39. Watanabe S., Noda T., Halfmann P., Jasenosky L. and Kawaoka Y. Ebola virus (EBOV) VP24 inhibits transcription and replication of the EBOV genome. *J Infect Dis*. 2007; 196, S284–S290. <https://doi.org/10.1086/520582> PMID: [17940962](https://pubmed.ncbi.nlm.nih.gov/17940962/)
 40. Hartman A.L., Towner J.S. and Nichol S.T. A C-terminal basic amino acid motif of Zaire ebolavirus VP35 is essential for type I interferon antagonism and displays high identity with the RNA-binding domain of another interferon antagonist, the NS1 protein of influenza A virus. *Virology*. 2004; 328, 177–184. <https://doi.org/10.1016/j.virol.2004.07.006> PMID: [15464838](https://pubmed.ncbi.nlm.nih.gov/15464838/)
 41. Leung D.W., Shabman R.S., Farahbakhsh M., Prins K.C., Borek D.M., Wang T.J., et al. Structural and functional characterization of Reston Ebola virus VP35 interferon inhibitory domain. *J Mol Biol*. 2010; 399, 347–357. <https://doi.org/10.1016/j.jmb.2010.04.022> PMID: [20399790](https://pubmed.ncbi.nlm.nih.gov/20399790/)
 42. Guito J.C., Albarino C.G., Chakrabarti A.K. and Towner J.S. Novel activities by ebolavirus and marburgvirus interferon antagonists revealed using a standardized in vitro reporter system. *Virology*. 2017; 501, 147–165. <https://doi.org/10.1016/j.virol.2016.11.015> PMID: [27930961](https://pubmed.ncbi.nlm.nih.gov/27930961/)
 43. Prins KC, Cardenas WB, Basler CF. Ebola virus protein VP35 impairs the function of interferon regulatory factor-activating kinases IKKepsilon and TBK-1. *J Virol*. 2009; 83(7):3069–77. <https://doi.org/10.1128/JVI.01875-08> PMID: [19153231](https://pubmed.ncbi.nlm.nih.gov/19153231/)
 44. Luthra P, Ramanan P, Mire CE, Weisend C, Tsuda Y, Yen B, et al. Mutual antagonism between the Ebola virus VP35 protein and the RIG-I activator PACT determines infection outcome. *Cell Host Microbe*. 2013; 14(1):74–84. <https://doi.org/10.1016/j.chom.2013.06.010> PMID: [23870315](https://pubmed.ncbi.nlm.nih.gov/23870315/)
 45. Leung D.W., Ginder N.D., Fulton D.B., Nix J., Basler C.F., Honzatko R.B. et al. Structure of the Ebola VP35 interferon inhibitory domain. *Proc Natl Acad Sci U S A*. 2009; 106, 411–416. <https://doi.org/10.1073/pnas.0807854106> PMID: [19122151](https://pubmed.ncbi.nlm.nih.gov/19122151/)
 46. Aswad A. and Katzourakis A. Paleovirology and virally derived immunity. *Trends in ecology & evolution*. 2012; 27, 627–636. <https://doi.org/10.1016/j.tree.2012.07.007> PMID: [22901901](https://pubmed.ncbi.nlm.nih.gov/22901901/)
 47. Bannert N. and Kurth R. (2004). Retroelements and the human genome: New perspectives on an old relation. *Proc Natl Acad Sci U S A*. 101, 14572–14579. <https://doi.org/10.1073/pnas.0404838101> PMID: [15310846](https://pubmed.ncbi.nlm.nih.gov/15310846/)
 48. Stoye J.P. Studies of endogenous retroviruses reveal a continuing evolutionary saga. *Nat Rev Microbiol*. 2012; 10, 395–406. <https://doi.org/10.1038/nrmicro2783> PMID: [22565131](https://pubmed.ncbi.nlm.nih.gov/22565131/)
 49. Leroy E.M., Kumulungui B., Pourrut X., Rouquet P., Hassanin A., Yaba P., et al. Fruit bats as reservoirs of Ebola virus. *Nature*. 2005; 438, 575–576. <https://doi.org/10.1038/438575a> PMID: [16319873](https://pubmed.ncbi.nlm.nih.gov/16319873/)
 50. Pourrut X., Souris M., Towner J.S., Rollin P.E., Nichol S.T., Gonzalez J.P. et al. Large serological survey showing cocirculation of Ebola and Marburg viruses in Gabonese bat populations, and a high seroprevalence of both viruses in *Rousettus aegyptiacus*. *BMC Infect Dis*. 2009; 9, 159. <https://doi.org/10.1186/1471-2334-9-159> PMID: [19785757](https://pubmed.ncbi.nlm.nih.gov/19785757/)
 51. Yuan J., Zhang Y., Li J., Zhang Y., Wang L.-F. and Shi Z. Serological evidence of ebolavirus infection in bats, China. *Virol J*. 2012; 9, 236. <https://doi.org/10.1186/1743-422X-9-236> PMID: [23062147](https://pubmed.ncbi.nlm.nih.gov/23062147/)

52. Ogawa H., Miyamoto H., Nakayama E., Yoshida R., Nakamura I., Sawa H., et al. Seroepidemiological prevalence of multiple species of filoviruses in fruit bats (*Eidolon helvum*) migrating in Africa. *J Infect Dis.* 2015; 212, S101–S108. <https://doi.org/10.1093/infdis/jiv063> PMID: 25786916
53. Swanepoel R., Leman P.A., Burt F.J., Zachariades N.A., Braack L.E.O., Ksiazek T.G., et al. Experimental inoculation of plants and animals with Ebola virus. *Emerg Infect Dis.* 1996; 2, 321–325. <https://doi.org/10.3201/eid0204.960407> PMID: 8969248
54. Larkin M.A., Blackshields G., Brown N., Chenna R., McGettigan P.A., McWilliam H. et al. Clustal W and Clustal X version 2.0. *Bioinformatics.* 2007; 23, 2947–2948. <https://doi.org/10.1093/bioinformatics/btm404> PMID: 17846036
55. Niwa H., Yamamura K. and Miyazaki J. Efficient selection for high-expression transfectants with a novel eukaryotic vector. *Gene.* 1991; 108, 193–199. PMID: 1660837
56. Talon J., Horvath C.M., Polley R., Basler C.F., Muster T., Palese P. and Garcia-Sastre A. Activation of interferon regulatory factor 3 is inhibited by the influenza A virus NS1 protein. *J Virol.* 2000; 74, 7989–7996. <https://doi.org/10.1128/JVI.74.17.7989-7996.2000> PMID: 10933707
57. Kawai T., Takahashi K., Sato S., Coban C., Kumar H., Kato H., et al. IPS-1, an adaptor triggering RIG-I- and MDA5-mediated type I interferon induction. *Nat Immunol.* 2005; 6, 981–988. <https://doi.org/10.1038/ni1243> PMID: 16127453
58. Changula K., Yoshida R., Noyori O., Marzi A., Miyamoto H., Ishijima M., et al. Mapping of conserved and species-specific antibody epitopes on the Ebola virus nucleoprotein. *Virus Res.* 2013; 176, 83–90. <https://doi.org/10.1016/j.virusres.2013.05.004> PMID: 23702199
59. R Core Team (2015). R: A Language and Environment for Statistical Computing. R Foundation for Statistical Computing, Vienna, Austria. URL <https://www.R-project.org/>.